Supporting Information

Mechanically Alloyed $CdGeP_2$ Coupled with Optimized Conductive Frameworks for Ultrafast Lithium Storage

Zedong Li[a,1], Wei Pan[b,1], Yuanxia Zhang[a], Hongming Zhang[a], Haipeng Wang[a], Pengfei Hou[a], Xinxin Wang[a], Jingjing Chen[a], Chenlong Dong[a,b,*] and Zhiyong Mao[a,b,*]

[a] Tianjin Key Laboratory for Photoelectric Materials and Devices, School of Materials Science and Engineering, Tianjin University of Technology, Tianjin 300384, PR China

[b] School of Electrical Engineering and Automation, Tianjin University of Technology, Tianjin 300384, PR China

[1] These authors contributed equally to this work.

Email: mzhy1984@163.com (Prof. Zhiyong Mao), dongchenlong@email.tjut.edu.cn (Assoc. Prof. Chenlong Dong)

Experimental Section

Preparation of metallic phosphides

The $CdGeP_2$ anode was synthesized by mechanochemical method *via* high-energy ball milling (HEBM). Stoichiometric amounts of Cd particle (Macklin, 99.99%), Ge powder (Macklin, 99.99%), and red P particle (Macklin, 99.5%) were ground by mortar and pestle and then loaded into a stainless-steel milling jar with stainless-steel balls (ball-to-powder ratio: 25). The jar was sealed in Ar-filled glovebox to prevent oxidation. The milling process was carried out using a high-energy planetary ball mill (MSK-SFM-3, Hefei Kejing Materials Technology Co., Ltd.) at a fixed rotating speed of 1200 rpm for 12 h (a half-hour break every two hours). The CdP_2 and GeP_2 reference samples were synthesized individually by adding the corresponding single metal source.

Synthesis of phosphides/carbon composites

To fabricate the carbon-composited materials, the as-synthesized phosphides were first homogeneously mixed with various carbonaceous materials, and then ball-milled for 2 h at a rotating speed of 1200 rpm (ball-to-powder ratio: 25) under Ar protection. The carbonaceous materials included acetylene black (AB), carbon nanotubes (CNTs) and graphene oxide (GO). The mass ratio of phosphides to the carbonaceous material was fixed at 7:2.

Materials Characterizations

X-ray diffraction (XRD) patterns were acquired on an ARL EQUINOX 3000 diffractometer (Thermo Fisher Scientific) employing Cu Kα radiation (λ = 0.15406 nm) to obtain the crystal structure information, with data collected over a 2θ range from 10° to 80°. The microstructure was examined using scanning electron microscopy (SEM, Quanta FEG, USA). The composition and crystal phase were further investigated by transmission electron microscopy (TEM) on a JEOL JEM-F200 instrument equipped with the ability to collect elemental information in high angle annular dark field-scanning transmission electron microscopy (HAADF-STEM) mode. X-ray photoelectron spectroscopy (XPS) measurements were performed on an Axis Ultra spectrometer (Kratos Analytical) with Al Kα monochromatic radiation (hν = 1486.7 eV) to determine the elemental valence states, and all binding energies were referenced to the adventitious carbon C 1s peak at 284.8 eV.

Electrochemical measurements

The anode slurry was prepared by homogenously mixing the active material, acetylene black, and polyvinylidene fluoride (PVDF) binder in a mass ratio of 7:2:1, using N-methyl-2-pyrrolidone (NMP) as the solvent. This resultant slurry was subsequently coated onto a Cu current collector employing a doctor-blade technique. The coated electrode was then dried overnight at 80°C. The dried electrode was punched into Φ 12 mm discs with an active mass loading of ~1.3 mg cm^{-2}. CR2016-type half-cells were assembled in an argon-filled glovebox, where the concentrations of H_2O and O_2 were maintained below 0.01 ppm. A Li foil served as both the counter and reference electrode, while a glass fiber membrane (Whatman) was used as the separator. The electrolyte used was 1 M $LiPF_6$ in a mixture of ethylene carbonate (EC) and diethyl carbonate (DEC) (*w/w*, 1:1) with 10 *wt.*% fluoroethylene carbonate (FEC) and 1 *wt.*% vinylene carbonate (VC) as additives. The galvanostatic charge/discharge tests for cyclic and rate performance evaluations were conducted on a LAND CT2001A battery test system within a potential window of 0.01–2.0 V (*vs.* Li/Li^+) at ambient temperature. Cyclic voltammetry (CV) and electrochemical impedance spectroscopy (EIS) measurements were performed using a CHI 760E electrochemical workstation (Shanghai Chenhua Technology Co., Ltd.). The CV tests were carried out between 0.01 and 2 V (*vs.* Li/Li^+) at different scan rates. EIS spectra were acquired in the frequency range from 100 kHz to 0.01 Hz with an amplitude of 5 mV. The galvanostatic intermittent titration technique (GITT) was employed by involving a constant current pulse of 0.05 A g^{-1} for 30 min followed by a relaxation step for 60 min. The cathode slurry was prepared by homogenously mixing the $LiFePO_4$ (LFP), acetylene black, and PVDF binder in a mass ratio of 8:1:1 using NMP as the solvent. Coin-type full cell ((+) LFP||$CdGeP_2$/GO (–)) was assembled by applying LFP cathode and $CdGeP_2$/GO anode with a N/P ratio of 1.1. Before assembling, the $CdGeP_2$/GO anode was pre-cycled for 3 cycles.

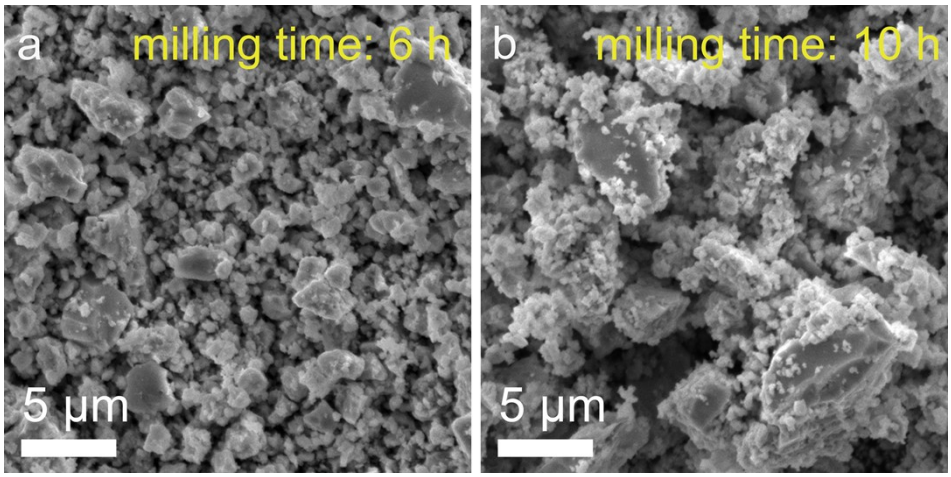

Figure S1. SEM images of $CdGeP_2$ samples ball-milled for (a) 6 and (b) 10 h.

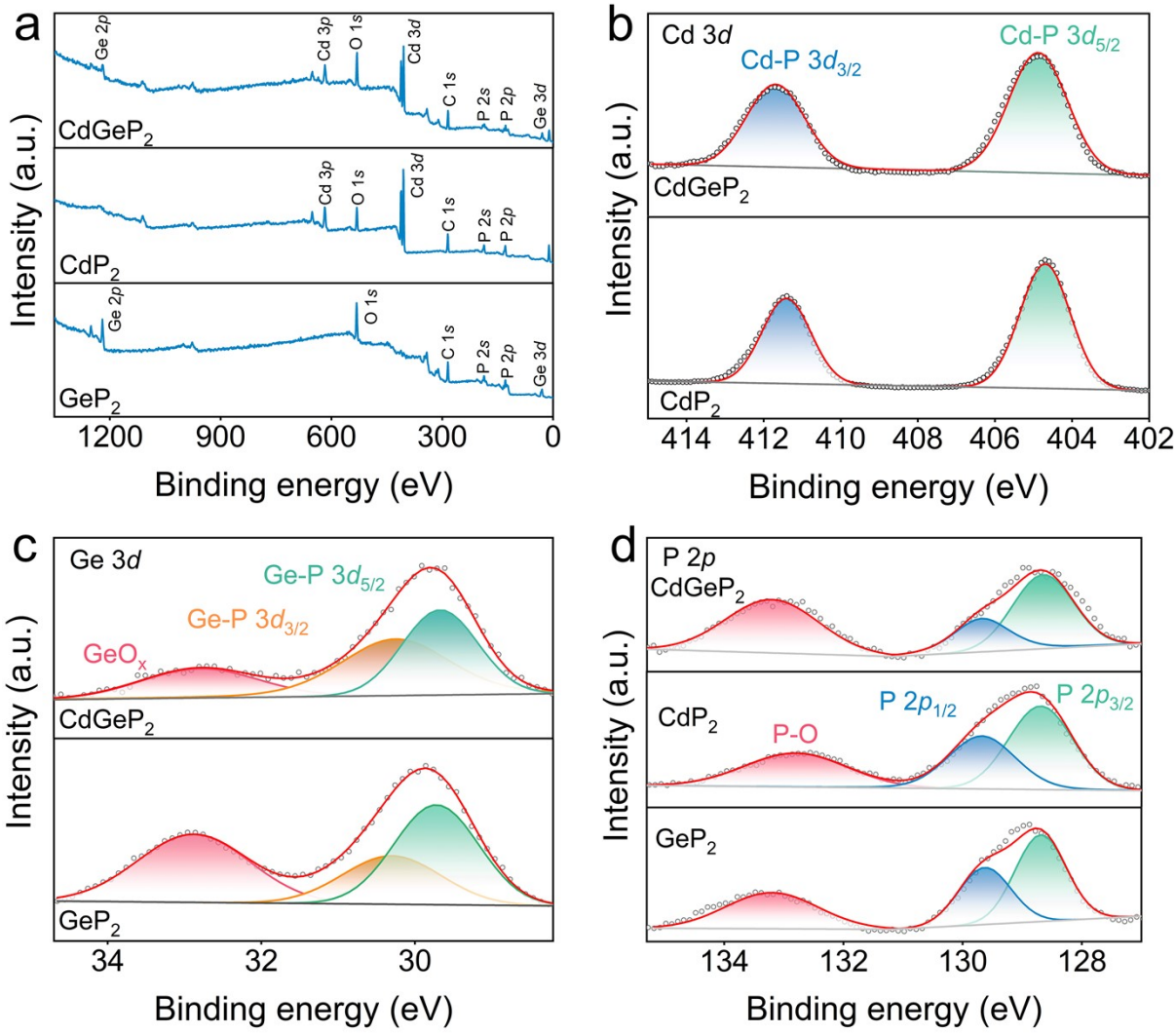

Figure S2. (a) XPS survey spectra of $CdGeP_2$, CdP_2 and GeP_2. High-resolution (b) Cd 3*d*, (c) Ge 3*d* and (d) P 2*p* spectra of $CdGeP_2$, CdP_2 and GeP_2.

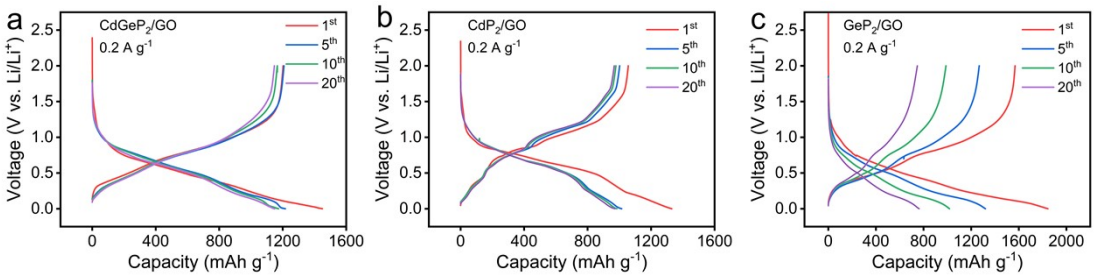

Figure S3. GCD curves of (a) $CdGeP_2$/GO, (b) CdP_2/GO and (c) GeP_2/GO within 20 cycles at 0.2 A g^{-1}.

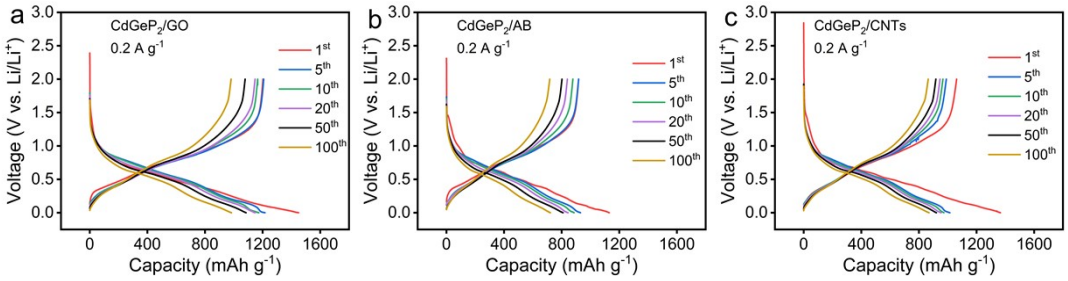

Figure S4. GCD curves (a)$CdGeP_2$/GO, (b) $CdGeP_2$/AB and (c) $CdGeP_2$/CNTs within 100 cycles at 0.2 A g^{-1}.

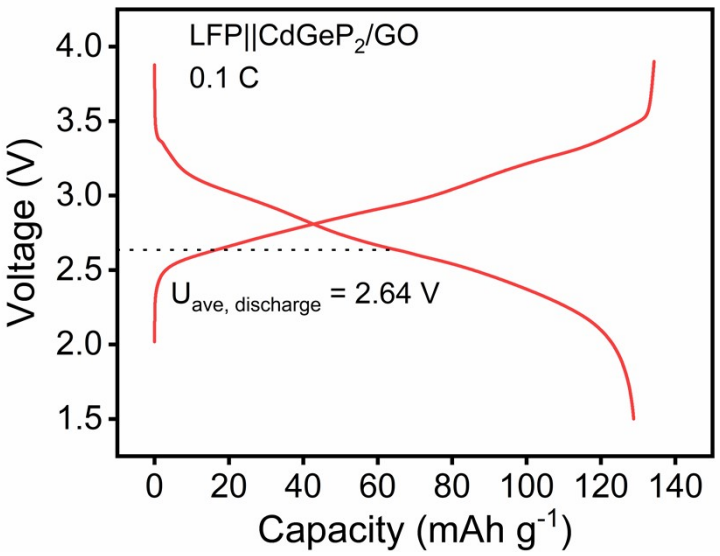

Figure S5. GCD curves of LFP||$CdGeP_2$/GO at the 1st cycle at 0.1 C within 1.5–3.9 V (1 C = 125 mA g^{-1}).

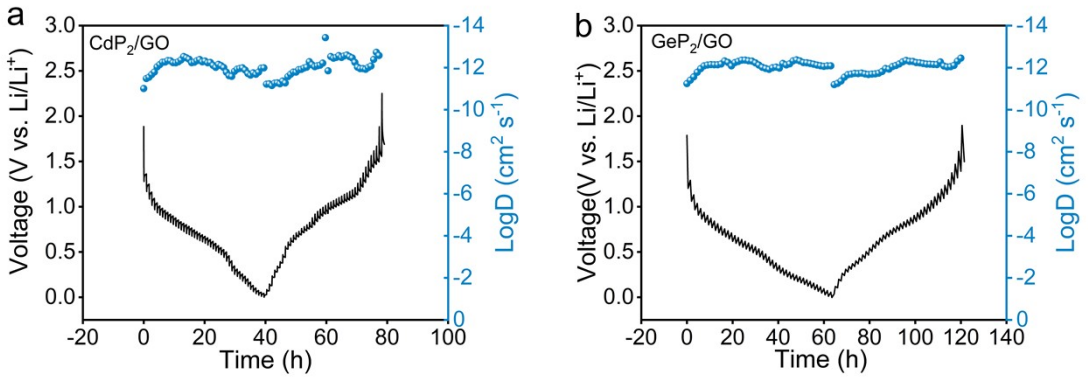

Figure S6. GITT curves of (a) CdP_2/GO and (b) GeP_2/GO anodes and corresponding D_{Li+} at various potentials.

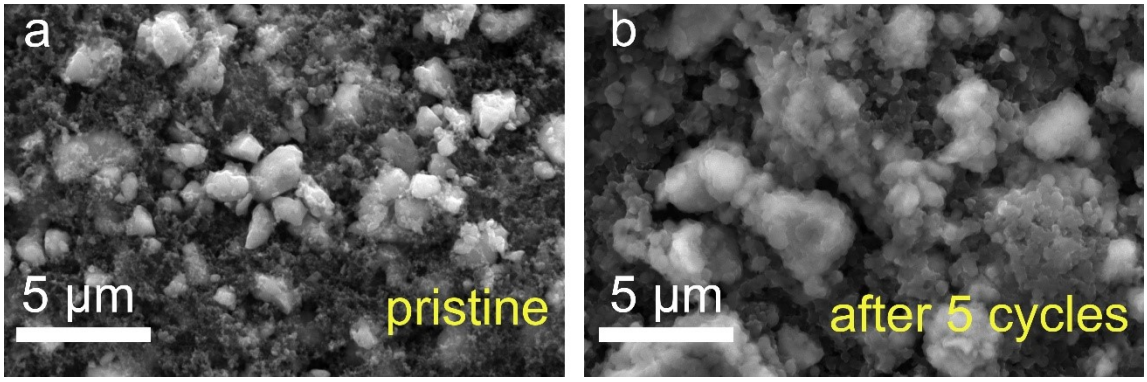

Figure S7. SEM images of the $CdGeP_2$/GO electrode (a) before and (b) after 5 cycles.

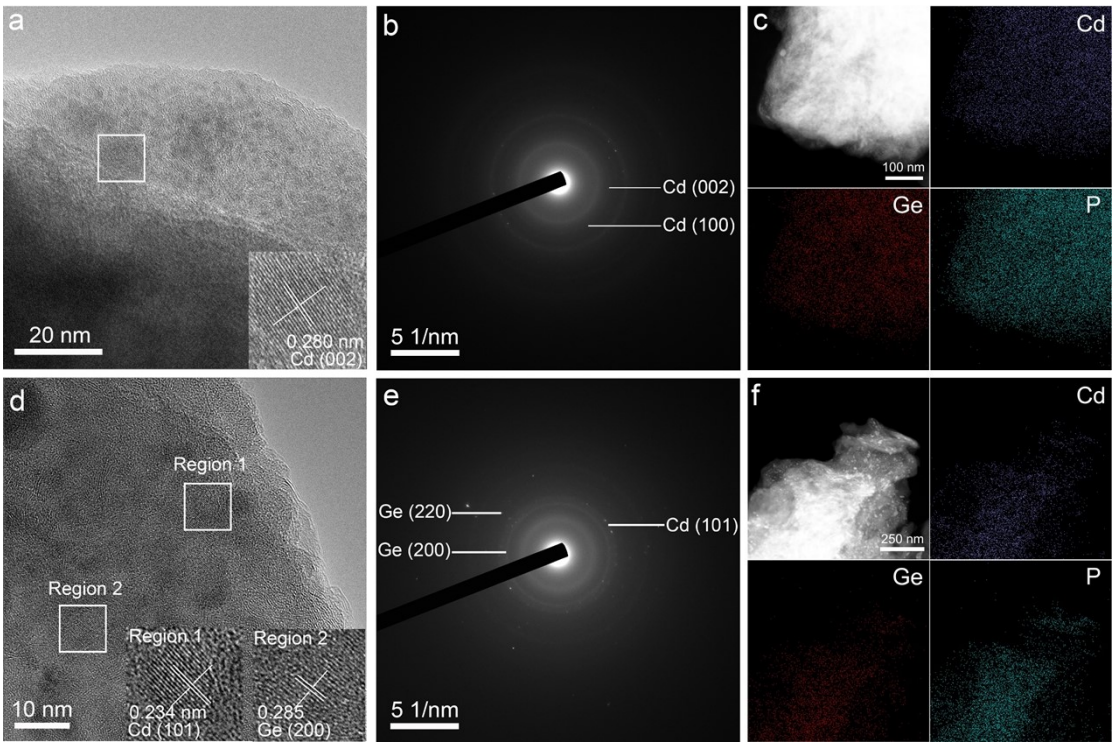

Figure S8. (a) *Ex situ* HRTEM, (b) SAED and (c) EDS mapping of $CdGeP_2$/GO electrode at 0.7 V. (d) *Ex situ* HRTEM, (e) SAED and (f) EDS mapping of $CdGeP_2$/GO electrode at 0.2 V.

Table S1. Comparison of electrochemical performance between $CdGeP_2$/GO and Cd-based, Ge-based, and P-based anodes.

Materials	Capacity at low current (mAh g^{-1}@A g^{-1})	Capacity at high current (mAh g^{-1}@A g^{-1})	Capacity (mAh g^{-1})@cycles@current (A g^{-1})	Ref.
CdO/CNTs	1100@0.1	720@1.5	810@100@0.1	1
Ge_3N_4@C	721.9@0.1	288.3@2	841.6@50@0.1	2
GeP_3/C	1235@0.1	753@3 C(1 C=950 mAh g^{-1})	845@100@0.1	3
SiGe	2362@0.2	666@1	590@100@0.2	4
FeP@C	825.7@0.1	416.5@5	902.4@100@0.1	5
FeP/SnP@C	1140.7@0.2	539@2	756.1@200@0.2	6
Co_3O_4@CdS	1292@0.1 C (1 C=891 mA h g^{-1})	258@5 C	760@200@0.1 C	7
$CdGeP_2$/GO	1449.9@0.2	576.5@10 369.9@15 156.2@20	981.5@100@0.2 674.4@500@1 374.8@500@10	This work

References

1. Feng, J., et al. Synthesis of nanosized cadmium oxide (CdO) as a novel high capacity anode material for lithium-ion batteries: influence of carbon nanotubes decoration and binder choice. *Electrochim. Acta* 129 (2014): 107-112.
2. Wu, Y., et al. Facile synthesis of Ge_3N_4@C nanostructures for high-performance lithium-ion batteries. *J. Energy Storage* 132 (2025): 117754.
3. Nam, K.-H., et al. Layered germanium phosphide-based anodes for high-performance lithium- and sodium-ion batteries. *Energy Storage Mater*. 17 (2019): 78-87.
4. Xiao, W., et al. Electrolytic Formation of Crystalline Silicon/Germanium Alloy Nanotubes and Hollow Particles with Enhanced Lithium-Storage Properties. *Angew. Chem*. 128 (2016): 7553-7557.
5. Zhang, X., et al. Shuttle-like carbon-coated FeP derived from metal-organic frameworks for lithium-ion batteries with superior rate capability and long-life cycling performance. *Carbon* 143 (2019): 116-124.
6. Li, J., et al. Long-Lasting Lithium-Ion Batteries Enabled by Advanced Anode Design of a Hydrangea-like FeP/SnP@C Heterostructure. *ACS Appl. Mater. Interfaces* 17 (2025): 12085-12094.
7. Waleed, H., et al. Mesoporous Co_3O_4@CdS nanorods as anode for high-performance lithium ion batteries with improved lithium storage capacity and cycle life. *RSC Adv*. 14 (2024): 11900-11907.